Reports

Atomic-Resolution Microscopy in Water

RICHARD SONNENFELD AND PAUL K. HANSMA

The scanning tunneling microscope is revolutionizing the study of surfaces. In ultrahigh vacuum it is capable not only of imaging individual atoms but also of determining energy states on an atom-by-atom basis. It is now possible to operate this instrument in water. Aqueous optical microscopy is confined to a lateral resolution limit of about 2000 angstroms, and aqueous x-ray microscopy has yielded a lateral resolution of 75 angstroms. With a scanning tunneling microscope, an image of a graphite surface immersed in deionized water was obtained with features less than 3 angstroms apart clearly resolved. Further, an image measured in saline solution demonstrated that the instrument can be operated under conditions useful for many biological samples.

A SCANNING TUNNELING MICROscope (STM) can provide images of atomic-scale features on surfaces. Atomic features on the surfaces of several crystalline semiconductors and evaporated metal films (*1–6*) have been resolved with this technique, and it has also been applied to the study of surface roughness (*7*), superconductivity (*8*), charge density waves (*9*), and biological specimens doped onto a graphite surface (*10*).

Since the time of Hooke (*11*) and Leeuwenhoek (*12*), most microscopic studies in aqueous environments have been done with optical microscopes, which are limited in lateral resolution to about 2000 angstroms (Å). Acoustic microscopes have many advantages (*13*), but their lateral resolution in water is comparable to that of optical microscopes. In an image of a living cell (*14*), a lateral resolution of 75 Å has been achieved with an x-ray microscope, and in the future, x-ray microscopes may give lateral resolutions of 10 Å (*14*). Modern electron microscopes, despite their enormous power, have been limited to the study of samples in a vacuum. Tunneling microscopes are more versatile in this respect. They have been operated in ultrahigh vaccuum, in air, and with the microscope and sample immersed in electrically insulating fluids such as paraffin oil and liquid nitrogen (*9, 15*).

We present here two images that illustrate a new capability for tunneling microscopes: operation with the sample immersed in water. The first image, in which features that are 2.46 Å apart are resolved, is of the surface of highly oriented pyrolytic graphite (*16*). The second is of the surface of an evaporated gold film. These samples were chosen for this initial test of tunneling microscopy in water for two reasons: i) they had been characterized in other environments with other tunneling microscopes, and ii) they could serve as substrates in future investigations of biological molecules and of processes that occur only in water.

To obtain an STM image in constant-current mode, a sharp tip attached to the z-axis of a micropositioner is brought within a few angstroms of the sample surface—so close that a small constant voltage applied between tip and sample produces a current, which is due to electrons tunneling across the gap. This current decreases by an order of magnitude if the gap between tip and sample increases by an atomic diameter. It is held constant by adjusting the z-axis of the micropositioner while the tip is raster-scanned with the x- and y-axes of the micropositioner. The image is formed from the record of vertical position required to keep the tunneling current constant as a function of x and y positions (*17–19*).

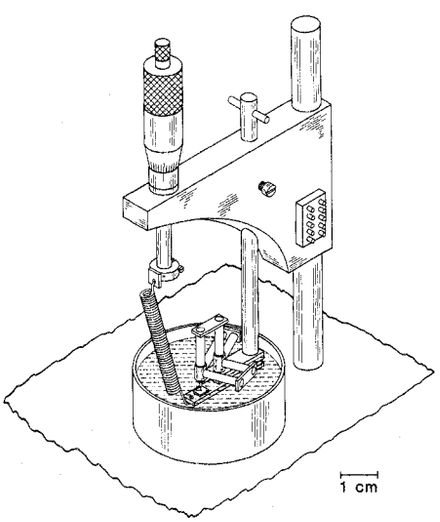

Fig. 1. The STM used in this research. The sample and sharp platinum-iridium tip were immersed in water while the x, y, and z tubular piezoelectric elements were above the surface of the water. The micrometer provided a fine adjust of the sample-to-tip distance.

Our microscope (Fig. 1) used three orthogonal pairs of piezoelectric tubes (Vernitron PZT-4) in the three-axis micropositioner. The two tubes in each pair had their polarization axes oppositely oriented. Thus, the tip was moved toward the surface by applying a voltage that caused the rear tube (clamped on a block referenced to the surface) to contract and the front tube (attached by a plate to the rear tube and also to the point) to expand. This double tripod arrangement provided almost the same amount of maximum travel (2800 Å) as a single tripod with double the tube length, but it also provided greater structural rigidity and first order cancellation of thermal drift. The microscope was designed such that the piezoelectric elements were kept out of the water, since these operated at voltages up to 100 V. The electronics were the same as in our earlier experiments (*15*), except that the series resistance we used to measure the tunneling current was 100 kilohms instead of 1 megohm, which allowed us to operate the tunnel junction at a lower resistance than before (*15*). The sample was mounted on a stainless steel plate, which was bent by a screw to bring the sample surface to within 10 μm of the tip. Once this coarse adjustment was completed, the STM was lowered into a plastic 100-ml beaker until the sample was about 1 mm below the surface of the water. A micrometer attached to the plate by a spring was then adjusted to bring the sample within tunneling range of the tip (1 mm of micrometer travel corresponded to roughly 1 μm of sample travel).

The tip was a platinum-iridium needle mounted in a stainless steel collar in the microscope. The diameter of the needle was 127 μm, and the needle projected 1 mm beyond the collar. The needles we used were a commercial product (*20*) for intracellular recording and were completely covered with glass insulation, except for about 50 μm at the tip where the insulation was removed. The primary function of the insulation was to minimize the area of the tip that could conduct current through the water and into the sample surface. The needles were also insulated from the grounded stainless steel collar, which acted as an electrostatic shield and greatly reduced capacitive pick-up by the needles of scan voltages applied to the piezoelectric elements.

An image of a graphite surface under deionized water is presented in Fig. 2. It is a Polaroid photograph of the raw data appearing on a storage oscilloscope screen.

Department of Physics, University of California, Santa Barbara, CA 93106.

The image was taken with the tip biased at −100 mV with respect to the surface. The set current was 50 nanoamperes (nA), of which 31 nA was due to tunneling current and the rest was due to ohmic conduction through ions in the water. Ohmic conduction was relatively constant over the 20 seconds necessary to produce this image (we could simply back the tip out of tunneling range and then read the conduction current through the water on the current monitor). If the conduction current dominated the tunneling current, the feedback loop stopped tracking the surface correctly.

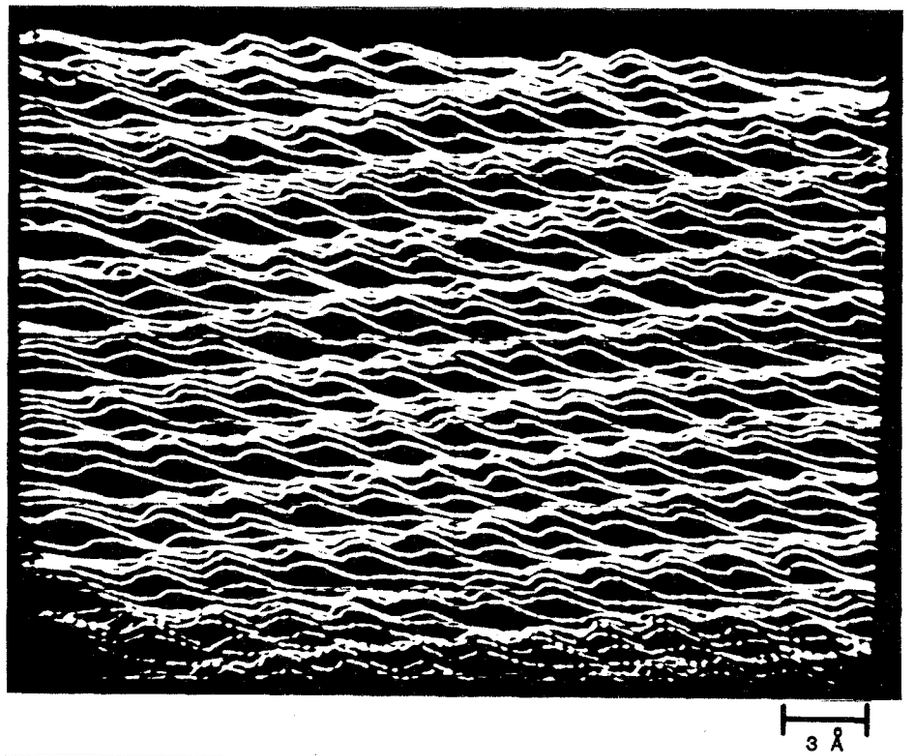

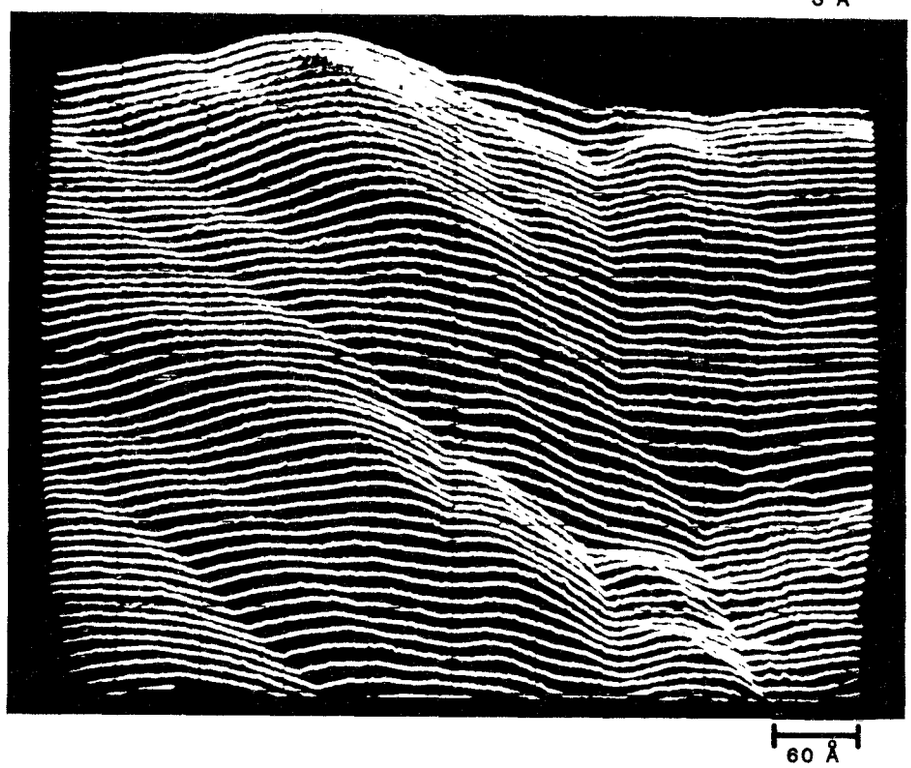

Fig. 2 (top). An STM image of a graphite surface immersed in water. The lattice visible in this image has hexagonal symmetry, which can be seen by noting that the features line up in rows along three axes separated by about 120 degrees. The imaging process emphasized the rows at a slight angle to horizontal and the rows falling at about 45 degrees from upper left to lower right. A third set of rows may be seen that is nearly vertical but slopes to the right from bottom to top. Fig. 3 (bottom). Lower magnification STM image of a gold film immersed in a 2 m*M* NaCl solution.

The observed structure is similar to that observed by Binnig *et al.* (*21*) in ultrahigh vacuum, by Park *et al.* (*22*) in air, and by our own group (*23*) in air. Most significantly, we see a simple hexagonal lattice of features. The hexagonal symmetry can most easily be seen by noting that the features line up in rows along three axes separated by about 120 degrees.

Though at first glance this may appear to be a lattice of rounded peaks, it is more consistent with theory to make the complementary statement: this is a lattice of rounded valleys. The atoms on a cleaved graphite surface are located at the vertices of the hexagons of a two-dimensional honeycomb. For tunnel-junction biases that are small compared to E_{Fermi}/e^-, theory and experiment concur that the largest observable effect is a valley in the electron-poor region at the center of each hexagonal ring. In turn, these valleys form a hexagonal close-packed structure. The periodicity of this lattice of valleys has been determined by theory and experiment to be 2.46 Å. This is consistent with (roughly 30 percent less than) an upper limit we obtained from a calculation that assumed complete polarization of the piezoelectric elements and no load imposed by the tubes of the STM at right angles to the direction of motion. The height of the structure was predicted to be 0.7 to 1 Å (*24*), whereas our structure appears to be 2.5 Å in height. These enhanced heights are not yet understood, but they have also been observed by others (*21*), and new theoretical work explicitly predicts them (*25*). The slight elongation of the hexagonal lattice could be attributed to thermal and electromechanical drifts in the STM and to a possible slight mismatch in the calibration of the *x* and *y* translators. The qualitative agreement with theory and the agreement with experiments in ultrahigh vacuum and air convince us that we are indeed resolving atomic-scale structures on a sample in an aqueous environment.

We obtained 18 atomic-resolution images of graphite in 3 days of operation. Roughly 10 percent of our time was spent obtaining the images, and 90 percent was spent (i) peeling off the top layers of the graphite to reveal fresh surfaces, (ii) searching with the *x*- and *y*-axes of the micropositioner for flat regions on the surface, and, if necessary, (iii) modifying the tip by touching it to the surface with the *z*-axis of the micropositioner, by cleaning it with a cotton swab

moistened with ethanol, or by gently sanding it with sandpaper (number 600).

Figure 3 is a lower magnification image of a gold film immersed in 2 m*M* NaCl. Our intent was to approximate the ionic concentration of a dilute solution of DNA. Images of this magnification were obtained routinely; we obtained more than 100 in a few days.

Gold depositions took place in a diffusion-pumped chamber at 5×10^{-6} torr. The cleaned glass substrate (a number 2 cover slide) was exposed for 30 seconds to glow discharge and then coated with a 7-Å chromium underlayer to improve adhesion of the gold film. The gold was evaporated from resistively heated sources and deposited at a rate of 3 Å per second to a thickness of 1000 Å, as measured by a quartz crystal thickness monitor.

The use of water as a medium did not complicate the operation of the tunneling microscope after the problem of operating in the presence of parallel conduction was solved. No evidence of the aqueous environment is evident from the images themselves. This is consistent with experimental results in air, liquid nitrogen, and paraffin oil (*9, 15*), in which the environment had no obvious effect on the images of the surface studied. Since the scan rate was slow compared to molecular motion, one would expect any effects due to water molecules in the gap to have been time-averaged.

In conclusion, a tunneling microscope can be operated in an aqueous environment and yield high-resolution images. This technique could be applied in several disciplines. In electrochemistry, it could be used to image an electrode surface before and after electrodeposition and, more generally, to study electrode reactions as a function of the structures on the electrode surface (*26*). In biology, the possibilities include imaging DNA, proteins, and membranes in their active states. If these were successful, further goals could include direct observation of biological processes such as DNA replication, enzymatic catalysis, and membrane transport.

REFERENCES AND NOTES

1. G. Binnig and H. Rohrer, *Surf. Sci.* **126**, 236 (1983).
2. ———, Ch. Gerber, E. Stoll, *ibid.* **144**, 321 (1984).
3. G. Binnig, H. Rohrer, Ch. Gerber, E. Weibel, *Phys. Rev. Lett.* **50**, 120 (1983).
4. J. A. Golovchenko, *Bull. Am. Phys. Soc.* **30**, 251 (1985).
5. R. M. Feenstra and G. S. Oehrlein, *Appl. Phys. Lett.* **47**, 97 (1985).
6. H. J. Scheel, G. Binnig, H. Rohrer, *J. Cryst. Growth* **60**, 199 (1982).
7. R. Miranda *et al.*, *Appl. Phys. Lett.* **47**, 367 (1985).
8. S. A. Elrod, A. L. de Lozanne, C. R. Quate, *Appl. Phys. Lett.* **45**, 1240 (1984).
9. R. V. Coleman, B. Drake, P. K. Hansma, G. Slough, *Phys. Rev. Lett.* **55**, 394 (1985).
10. A. M. Baró *et al.*, *Nature (London)* **315**, 253 (1985).
11. R. Hooke, *Micrographia* (London, 1665; reprinted by Weinheim, New York, 1961).
12. A. V. Leeuwenhoek, *Arcana Natura Detecta* (Leiden, 1772).
13. C. F. Quate, *Phys. Today* **38**, 34 (August 1985).
14. M. Howells, J. Kirz, D. Sayre, G. Schmahl, *ibid.*, p. 22.
15. B. Drake *et al.*, *Rev. Sci. Instrum.*, in press.
16. The material was called Grade ZYA Graphite Monochromator and was purchased from Union Carbide Corporation, Carbon Products Division, Chicago, IL.
17. A. L. Robinson, *Science* **220**, 43 (1983).
18. ———, *ibid.* **225**, 1137 (1984).
19. G. Binnig and H. Rohrer, *Sci. Am.* **253**, 50 (August 1985).
20. Model 30-05-1, Frederick Haer & Co., Brunswick, ME.
21. G. Binnig *et al.*, *Europhys. Lett.* **1**, 31 (1986).
22. Sang-Il Park and C. F. Quate, *Appl. Phys. Lett.* **48**, 112 (1986).
23. P. K. Hansma, R. Sonnenfeld, J. Schneir, B. Drake, J. Hadzicki, *Bull. Am. Phys. Soc.* **30**, 309 (1985).
24. A. Selloni, P. Carnevali, E. Tosatti, C. D. Chen, *Phys. Rev. B* **31**, 2602 (1985).
25. J. Tersoff, in preparation.
26. A. T. Hubbard *et al.*, *J. Electroanal. Chem.* **168**, 43 (1984).

27. Supported by NSF grant DMR83-03623. We thank Ch. Gerber and G. Binnig for suggesting that it might be possible to use water, on the basis of their preliminary experiments with a drop, N. Garcia for suggesting a study of highly oriented pyrolytic graphite, and S. Lindsay for suggesting the use of a saline solution. We thank S. Alexander, D. Cannell, S. Chiang, B. Drake, H. Hansma, A. Hubbard, J. Israelchevili, M. Kullin, S. Morita, H. Rohrer, D. Salisbury, C. Schneiker, J. Schneir, and J. Tersoff for useful discussions and especially K. Dransfeld and C. Quate for their enthusiasm and encouragement.

23 December 1985; accepted 3 March 1986

Decrease in Deformation Rate Observed by Two-Color Laser Ranging in Long Valley Caldera

M. F. LINKER, J. O. LANGBEIN, A. MCGARR

After the January 1983 earthquake swarm, the last period of notable seismicity, the rapid rate of deformation of the south moat and resurgent dome of the Long Valley caldera diminished. Frequently repeated two-color laser ranging measurements made within a geodetic network in the caldera during the interval June 1983 to November 1984 reveal that, although the deformation accumulated smoothly in time, the rate of extension of many of the baselines decreased by factors of 2 to 3 from mid-1983 to mid-1984. Areal dilatation was the dominant signal during this period, with rates of extension of several baselines reaching as high as 5 parts per million per annum during the summer of 1983. Within the south moat, shear deformation also was apparent. The cumulative deformation can be modeled as the result of injection of material into two points located beneath the resurgent dome in addition to shallow right lateral slip on a vertical fault in the south moat.

DRAMATIC EPISODES OF RAPID crustal deformation (*1, 2*) and unusual patterns of seismicity and attenuation (*3*) demonstrate that Long Valley caldera, a center of rhyolitic and basaltic volcanism in eastern California (*4*) within a region of lithospheric extension (*5*), is a potential site for volcanic hazard (*6*). Because of the concern that continued crustal deformation may lead to a volcanic eruption (*7*), we installed a geodetic network with which to observe subtle changes in the pattern of deformation within the south moat and to a lesser degree across the resurgent dome (Fig. 1) by means of a portable two-color geodimeter (*8*). We present data from 707 measurements made in this network from June 1983 to November 1984 (*9*).

The dominant feature of the data (Fig. 2) is the substantial lengthening of most of the baselines. When averaged over the initial 4 months, the lengthening rates of five of the baselines exceeded 5 parts per million (ppm) per annum, which is more than an order of magnitude greater than typical rates observed along geodetic baselines in the environs of the San Andreas fault zone (*10, 11*).

Perhaps the most interesting aspect of the data is the reduction in the rate of deformation during the period of observation. This decrease can be seen readily on 6 of the 13 individual line-length time histories that sample the entire reporting period. These include Casa-Hot, Casa-Rodger, Casa-Lomike, Casa-Sewer, Miner-Tilla, and Miner-Shark (Fig. 2), whose rates of lengthening decreased by factors of 2 to 3 from mid-1983 to mid-1984. For these six baselines, the addition of quadratic terms to models of constant lengthening rate is statistically significant.

To characterize the spatial distribution of cumulative deformation, we estimated the net length change of those baselines for which sufficient data exist during the time interval mid-July 1983 to mid-August 1984. Table 1 lists the length changes together with the estimated standard deviations based on the conservative assumption that each length change is determined from only

U.S. Geological Survey, Menlo Park, CA 94025.